Hindawi
Advances in Materials Science and Engineering
Volume 2023, Article ID 9793712, 1 page
https://doi.org/10.1155/2023/9793712

Retraction

Retracted: Thermal Conductivity of Thermally Insulated Concretes in a Nuclear Safety Vessel of Reactor Vault: Experimental Interpretation

Advances in Materials Science and Engineering

Received 26 December 2023; Accepted 26 December 2023; Published 29 December 2023

This article has been retracted by Hindawi, as publisher, following an investigation undertaken by the publisher [1]. This investigation has uncovered evidence of systematic manipulation of the publication and peer-review process. We cannot, therefore, vouch for the reliability or integrity of this article.

Please note that this notice is intended solely to alert readers that the peer-review process of this article has been compromised.

Wiley and Hindawi regret that the usual quality checks did not identify these issues before publication and have since put additional measures in place to safeguard research integrity.

We wish to credit our Research Integrity and Research Publishing teams and anonymous and named external researchers and research integrity experts for contributing to this investigation.

The corresponding author, as the representative of all authors, has been given the opportunity to register their agreement or disagreement to this retraction. We have kept a record of any response received.

References

[1] M. Anish, T. Arunkumar, J. Jayaprabakar et al., "Thermal Conductivity of Thermally Insulated Concretes in a Nuclear Safety Vessel of Reactor Vault: Experimental Interpretation," *Advances in Materials Science and Engineering*, vol. 2022, Article ID 4493910, 12 pages, 2022.

Hindawi
Advances in Materials Science and Engineering
Volume 2022, Article ID 4493910, 12 pages
https://doi.org/10.1155/2022/4493910

Research Article

Thermal Conductivity of Thermally Insulated Concretes in a Nuclear Safety Vessel of Reactor Vault: Experimental Interpretation

M. Anish,[1] **T. Arunkumar**,[2] **J. Jayaprabakar**,[1] **Sami Al Obaid**,[3] **Saleh Alfarraj**,[4] **M. M. Raj**,[5] **and Assefa Belay**[6]

[1]*School of Mechanical Engineering, Sathyabama Institute of Science and Technology, Chennai 600119, Tamilnadu, India*
[2]*Department of Mechanical Engineering, CMR Institute of Technology, Bengaluru 560037, Karnataka, India*
[3]*Department of Botany and Microbiology, College of Science, King Saud University, P.O. Box-2455, Riyadh-11451, Saudi Arabia*
[4]*Zoology Department, College of Science, King Saud University, Riyadh 11451, Saudi Arabia*
[5]*Department of Mechatronics Engineering, Seoul National University of Science and Technology, Seoul 01811, Republic of Korea*
[6]*Department of Mechanical Engineering, MizanTepi University, Tepi, Ethiopia*

Correspondence should be addressed to Assefa Belay; assefa@mtu.edu.et

Received 6 March 2022; Accepted 3 May 2022; Published 21 June 2022

Academic Editor: Palanivel Velmurugan

Thermally insulated concretes are a type of alternative building material that helps improve thermal efficiency in nuclear reactor vault safety vessel applications. The experimental results of thermal conductivity values of lightweight concrete materials at various temperatures are presented in this paper. To minimize heat conduction in concrete, different lightweight aggregates and vermiculite are employed as coarse aggregate alternatives.Both linear and plane heat source approaches are used to calculate the thermal conductivity values of the specimens. The findings emphasize that increasing the proportion of lightweight particles in concrete may dramatically lower the thermal conductivity, with the kind of lightweight aggregates having a vital role in thermal insulation. The inclusion of micron-sized vermiculite decreases heat conductivity even further; however, the effect is less obvious than that of lightweight particles.

1. Introduction

Concrete is the major core material utilized in the building of the Nuclear Reactor Safety Vault, which acts as the last barrier against the reactor's high temperature heat waves and other fission products. Concrete's thermal conductivity is crucial for trapping heat and preventing it from dispersing into the surrounding environment. Because of their superior heat conductivity, thermally insulated concretes are chosen over standard concretes. This is performed by replacing coarse aggregates with appropriate lightweight aggregates. Pumice, coconut shell, and volcanic rock are the most common lightweight aggregates used in structural lightweight concretes. The addition of this LWA increases thermal insulation without compromising the mechanical qualities of the concrete. Density, conductivity, and diffusivity all fall by 50% at 900°C when compared to room temperature values. The specific heat grows steadily until 500°C, then decreases from 7000°C to 900°C, and then increases over 900°C [1–3]. LWAs' porosity accounts for more moisture absorption than standard aggregates, impacting the thermal properties of structural concrete [3, 4]. The 28-day compressive strength of concrete estimated using the coconut shell aggregate is 19.1 N/mm^2, which is higher than the standard requirement for structural lightweight concrete [5]. The thermal conductivity of concrete varies from 2.01 to 2.95 W/m/K depending on the aggregate [6]. Normal concrete's thermal conductivity ranges from 2.194 W/m/K to 1.027 W/m/K at temperatures ranging from 20°C to 1100°C [7]. According to the research, traditional concrete thermal

conductivity varies from 0.6 to 3.3 W/m/K, whereas lightweight concretes vary from 0.4 to 1.89 W/m/k [8]. Although lightweight concretes are classed as aerated concretes and lightweight aggregate concretes (LWA), the latter has higher strength and density as well as poorer thermal conductivity, in addition to requiring a high energy production method [9]. When used as a fine aggregate, pumice dramatically inhibits heat conductivity by up to 40% [10]. The thermal conductivity of aggregate is substantially impacted by the value of aggregate loose unit weight and the volume of the aggregate matrix to the total volume ratio [11]. The incorporation of fly ash in a certain proportion with water in the mix design enhances the strength of the concrete while lowering heat conductivity [12]. At temperatures ranging from 0°C to 50°C, normal concretes have a thermal conductivity of 0.7–0.8 W/m·K, whereas lightweight concretes have a thermal conductivity of 0.5–0.6 W/m·K. Because LWAC may be used for partition or barrier walls due to its high thermal diffusivity and low unit weight, porosity is one of the major parameters that directly impacts its thermal conductivity [13]. According to DCT testing results, an increase in moisture content has an influence on the mechanical characteristics of concrete [14]. Concrete cracking drastically lowered thermal conductivity while maintaining the same specific heat capacity [15]. Both the inner vault, which holds the primary vessel, and the outer vault, which holds the safety vessel, are cylindrical structures. The vault's temperature is limited to 65 degrees Celsius, despite the fact that the main vessel may reach temperatures of up to 5000 degrees Celsius. Temperatures in the Reinforced Inner and Outer vaults range between 500°C and 550°C and 65°C and 90°C, respectively [16]. Coconut shell aggregate concrete is well-known for its excellent bonding strength and long-term durability without losing quality [17]. Because of the high porosity values, both thermal conductivity and tensile strength are reduced. The degree of damage to concrete varies depending on the weight, lowering thermal conductivity [18]. The thermal conductivity of LWAC has been determined to be proportional to the volume of LWA. Thermal conductivity is lowered by 7% when pumice replaces 25% of coarse aggregates, and by 20%, 28%, and 47% when 50%, 75%, and 100% pumice aggregates are used, respectively. Thermal conductivity reduces from 0.96 to 0.65 W/m K.when 10% vermiculite is added and heated to 900°C. Mechanical strength and thermal conductivity increase [19]. Because the degree of strength depreciation is substantial at 400°C [20], concrete mechanical strength is directly proportional to the coarse aggregate. When 40% of the traditional aggregate is substituted with coconut shell, the concrete becomes lighter and the density is lowered by 7.5%. After 7 days, the strength of coconut shell concrete is significantly higher than that of control concrete. The water/cement ratio appeared to be affected by the amount of coconut shell utilized; as more cement was needed as the amount of coconut shell rose [21]. The k values of thermal insulating materials are tested in standard laboratory conditions. When a material is exposed to varying humidity and climatic conditions, its thermal performance changes dramatically [22]. Increasing the cement content without altering the workability of LWAC improves its resistance dramatically [23]. The purpose of this publication is to show how thermo-shielded structural concretes may be utilized in nuclear reactor safety vessels. The text is divided into two parts: Because of the use of lightweight aggregates and vermiculate, heat conductivity is reduced while strength is increased. Using a thermal needle probe in conjunction with the thermal moulding testing technique, thermal conductivity is evaluated. In addition, how this appropriate combination of concrete design will be improved in order to protect the nuclear safety vessel vault via the use of experimental analysis is also discussed.

Table 1: Physical properties of ordinary Portland cement and fly ash.

Properties	Cement	Fly ash
Sio_2 (%)	20.0	61.0
Loss on ignition (%)	2.6	2.5
Specific gravity (g/cm^3)	3.15	2.18
Blain fineness (cm^2/g)	3350	3308

Table 2: Physical properties of normal aggregates.

Properties	Fine	Coarse
Source	Cleaned sea-sand	Ballast
Fineness modulus	2.83	6.84
Specific gravity	2.60	2.61
Dry bulk density	1480	1680

2. Experiment

2.1. Primary Materials. Ordinary Portland cement, fly ash, GGBS (Ground Granulated Blast-furnace Slag), fine aggregate, coarse aggregates, and three lightweight coarse aggregates are the primary components [24]. Table 1 summarizes the characteristics of cement and fly ash. M40-sand that has been thoroughly washed and sieved is utilized as fine aggregates, whereas ballast is used as standard coarse aggregates as shown in Table 2. The fineness modulus of coarse aggregates is represented by an index value that indicates the average size of the particles included inside the coarse aggregate. It's estimated as part of the sieve analysis procedure, and it's done using conventional sieves. The value of fine aggregates may be calculated by adding together the cumulative percentage retained on each filter and dividing by 100.Pumice, volcanic rock, and crushed coconut shells are three diverse lightweight aggregates generated from various resources and procedures that are used as alternatives to typical coarse aggregates for enhancing thermal characteristics. Table 3 shows the physical parameters of lightweight aggregates. Micrometer-sized vermiculite is utilized as a substitute for aggregates. Vermiculite enhances thermal characteristics when combined with cement paste since it has a low thermal conductivity and density as shown in Table 4. The optical pictures of insulating LWA materials used for this study are shown in Figure 1.

Table 3: Mixture proportions.

Specimen	Cement (kg/m^3)	Fly ash (kg/m^3)	GGBS	Water (kg/m^3)	Aggregate			
					Fine (kg/m^3)	Coarse (kg/m^3)	Vermiculite (kg/m^3)	LWA (kg/m^3)
*N*0	350	0	0	150	818	1082	0	0
*N*5	280	52.5	17.5	150	777.1	1082	40.9	0
*N*10	280	52.5	17.5	150	736.2	1082	81.8	0
*N*20	280	52.5	17.5	150	654.4	1082	163.6	0
*N*30	280	52.5	17.5	150	572.6	1082	245.4	0
*P*0	280	52.5	17.5	150	818	898.06	0	183.94
*P*10	280	52.5	17.5	150	744.38	865.6	73.62	216.4
*P*20	280	52.5	17.5	150	728.02	843.96	89.98	238.04
*P*30	280	52.5	17.5	150	760.74	919.7	57.26	162.3
*V*0	280	52.5	17.5	150	818	865.6	0	216.4
*V*20	280	52.5	17.5	150	728.02	843.96	89.98	238.04
*C*0	280	52.5	17.5	150	818	865.6	0	216.4

Table 4: Properties of normal and lightweight coarse aggregates.

Properties	Normal	Pumice	Volcanic rock	Coconut shell
Raw material	Ballast	Volcanic	Volcanic	Coconut
Maximum size (mm)	20	20	15	12.5
Particle density (kg/m^3)	2500	300	710	650
Dry loose bulk density (kg/m^3)	1200	750	675	550
Shape type	Crushed	Crushed	Crushed	Flaky
Water absorption (%)	1	55	62	13.79

(a) (b) (c) (d)

Figure 1: Images of lightweight aggregates. (a) Vermiculite. (b) Pumice. (c) Volcanic rock. (d) Coconut shell.

2.2. Tested Specimens. Table 3 shows 10 possible aggregate and vermiculite blends with varied mix patterns. The specimen name is abbreviated with a symbol, which is then followed by a number. The number indicates the volume % of vermiculite added (i.e., *N*: normal aggregate, *P*: pumice, *V*: volcanic rock, and *C*: coconut shell) and the symbol indicates the kind of aggregate (i.e., *N*: normal aggregate, *P*: pumice, *V*: volcanic rock, and *C*: coconut shell) (i.e., *N*: normal aggregate, *P*: pumice, *V*: volcanic rock, and *C*: coconut shell). Table 3 shows the mix design of *N*0 for a structural insulated concrete used in a reactor with a compressive strength more than 27 MPa. The relative density and specific gravity of the components are considered when estimating the quantity of each item needed for a cubic metre of concrete. For example, the specimen is identified by the first letter of the primary ingredient, followed by the entire aggregate quantity of vermiculite to be replaced. The features and characteristics of normal and lightweight coarse aggregates are described in Tables 4 and 5, respectively.

Table 5: Specification of vermiculite.

Properties	Specifications
Composition	Phyllosilicates
Color	Light to dark brown
Density	160 kg/m^3
Crushed strength	0.56 mpa
Softening temperature	1200°c
Median diameter	50 μm
Bulk thermal conductivity	0.07 w/m/k

2.3. Making and Curing. For testing the compressive strength, a 150 mm × 150 mm × 150 mm cube is casted. A mold of size 300 mm × 300 mm × 300 mm is made to calculate the thermal conductivity. All cubes are de-moulded and cured in a tank at room temperature for 28 days (20 ± 3°C). Compressive strength, modulus of elasticity, density, and splitting tensile strength are measured after 28 days of curing. The thermal molds must be stored at room

temperature and 50% relative humidity for at least 14 days. Thermal conductivity is measured only after at least 28 days.

2.4. Measurement of Thermal Conductivity. The conventional approach for calculating thermal conductivity under adiabatic conditions is to measure the heat flux through the specimen, which requires a sophisticated experimental arrangement. In this work, three approaches are used: thermal needle probe method, thermal moulding method (one-dimensional and two-dimensional steady-state circumstances), and thermal moulding method (one-dimensional and two-dimensional steady-state conditions). Thermal conductivity is best measured under steady-state circumstances. The steady-state condition equation is as follows:

$$Q = k \cdot A \cdot t \cdot \frac{(T1 - T2)}{x}. \quad (1)$$

2.5. Thermal Needle Probe method. Two needle probes are used to generate heat during the concrete mixing process. A thermal needle probe is used to assess thermal conductivity. The thermistor and heating wire are integrated in a stainless steel needle probe 90 mm long and 1.3 mm in diameter. At the centre, two needle probes are introduced, followed by concrete mixing and hardening. Heat is created radially from the probe by employing DC current. For 2 minutes, the temperature is recorded every 1 second. Using equation (2), the linear part of temperature evolution with time is used to calculate thermal conductivity k.

$$k = \frac{Q}{4\pi}. \ln\left(\frac{\Delta t}{\Delta T}\right). \quad (2)$$

Q, applied heat energy. Δt, change in time. ΔT, change in temperature.

For each thermal probe, measurements are taken three times for two different input voltages (i.e., 10 and 15 V). Because the initial section of the temperature change is impacted by needle-concrete coupling, the conductivity is calculated from the linear portion temperature increment using a log time scale. The concrete mixes employed in this investigation comprise isotropic and homogenous components.

2.6. Thermal Molding Method. This method of heat transmission is preferred over the use of a thermal needle probe since the latter has a lower efficiency of heat transfer. Heating plates are used in this technique to transmit heat from the heating plate to the mould. In both one and two dimensions, the constant heat flow technique is utilized to calculate heat flow. In the one-dimensional heat flow method, just one heating plate is used, and the rest of the mould is completely insulated. When working with two-dimensional steady-state heat flow, two heating plates are placed on each side of the mould, opposing each other. The mould has been thermally insulated with asbestos sheeting in order to reduce the amount of heat lost. Figure 2 depicts the specimen layout as well as the thermocouple locations. A direct current is sent via the heating plates, which generates heat as a result. The heating plate equipment is composed of Nichrome coils that are put into porcelain grooves and covered by asbestos material to prevent heat dissipation during the heating process. The direct current (DC) supply that powers the heating plate equipment is 3 kilowatts. The nine thermocouples are arranged in a consecutive manner to measure temperature every 10 seconds. The heat propagation through the mould is monitored by the four thermocouples that have been put into the mould until the steady-state condition has been attained. Thermal moulding outperforms needle probe because heat is transmitted throughout the specimen by delivering planar heat across the specimen. Two heating plates are supplied in order to ensure that heat propagation is homogenous on both sides of the heating element. Thermal property is assessed using Fourier's law equation (3), which takes into account the loss of heat due to the atmosphere, thereby meeting the principle of energy conservation. For example, the total volume percentage of vermiculate relative to aggregates and the specific heat of the concrete sample are shown in Tables 6 and 7.

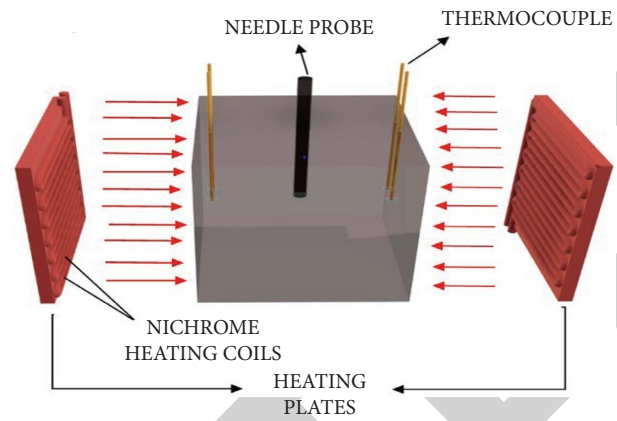

Figure 2: Thermal molding method: two-dimensional heat flow.

Table 6: Total volume fraction of vermiculate with respect to aggregates.

Notation	Volume of vermiculite (%)	
	Total aggregates	Coarse aggregates
5	4.8	15
10	9.7	28
20	19.6	51
30	29.5	78

Table 7: Specific heat of concrete specimens.

values (J/kg/k)	Material type
960	Concrete
920	Concrete
795	Normal weight concrete
921	Structural lightweight concrete
1000	Insulating lightweight concrete

$$\frac{dT}{dt} = \alpha \frac{dT}{dx} - \lambda.T, \\ = \frac{k}{\rho.c_p} \frac{dT}{dx} - \lambda.T^*, \quad (3)$$

α-, thermal diffusivity [m^2/s]. K, thermal conductivity [W/m/K]. c_p, specific heat [J/g/k]. &Rgr;, density [kg/m^3]. Heat loss coefficient, $\lambda = L/(dx.A.C_v.\rho)[1/S]$.

While the heat loss coefficient controls the steady-state temperature, the diffusivity monitors the rate of temperature rise. The change of temperature over time is analyzed using the finite difference approach, and equation (3) is amended. Thermal conductivity is measured using the specific heat and the density of the specimens, which are collected experimentally after 28 days of curing. According to Table 7, the average specific heat value for concrete is 890 J/kg/K. Thermal conductivity is calculated as a result. The heat loss coefficient and the projected thermal conductivity are independent, and they have no effect on temperature rise.

2.7. One-Dimensional Steady-State Condition. If the spatial distribution of temperatures in the conducting item does not change any more as the temperature difference driving the conduction remains constant, this form of conduction is said to be steady-state conduction. One-dimensional heat flow is applied when the heat energy flows along the coordinates normal to surface.

If k is a constant, then [4].

$$\frac{\partial T}{\partial x} + \frac{q}{k} = \frac{\rho c}{k} \frac{\partial T}{\partial t} = \frac{1}{\alpha} \frac{\partial T}{\partial t}, \quad (4)$$

$\partial T/\partial x$, longitudinal conduction. q, internal heat generation. $\partial T/\partial t$, thermal inertia. α, thermal diffusivity.

The concrete specimen is subjected to heat flow from just one side in this procedure, and the remaining sides are thermally insulated to decrease heat dispersion, as illustrated in Figure 3. Heat is applied to the concrete until a steady-state condition is reached. The temperature of the specimen is measured every two minutes for an hour. The temperature rise begins with the thermocouple closest to the heat source and continues in this manner. Temperature measurements are acquired by attaching thermocouples to the data logger system, and thermal conductivity is computed from the values using equation (4). Figure 4 shows the internal structure of the concrete vault.

3. Results and Discussion

From the prevailing effective factors, thermal needle probe and thermal molding methods are used to calculate thermal conductivity. The values from the one-dimensional steady-state method are analyzed with the recordings from the two methods to verify the experimental correctness. Results from the tested concrete specimen with various specifications are noted and further analyzed.

3.1. Effect of Lightweight Aggregates and Vermiculite. Figure 5 represents the thermal conductivity of normal concretes with varying amounts of vermiculite. A mean

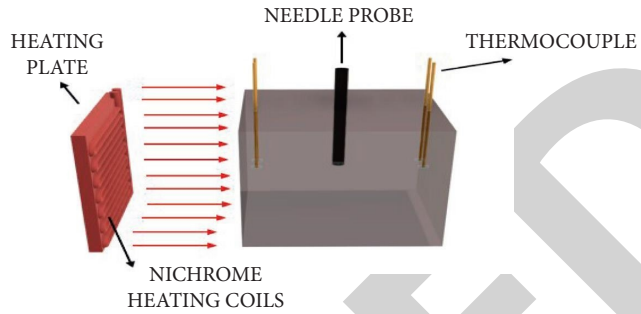

Figure 3: Thermal molding method: one-dimensional heat flow.

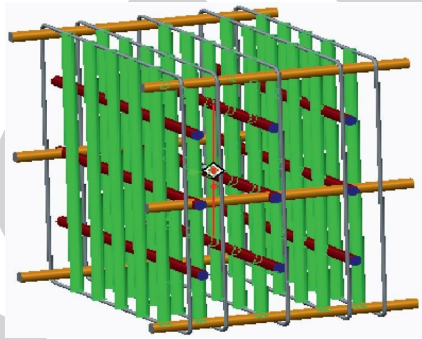

Figure 4: Internal structure of the concrete vault.

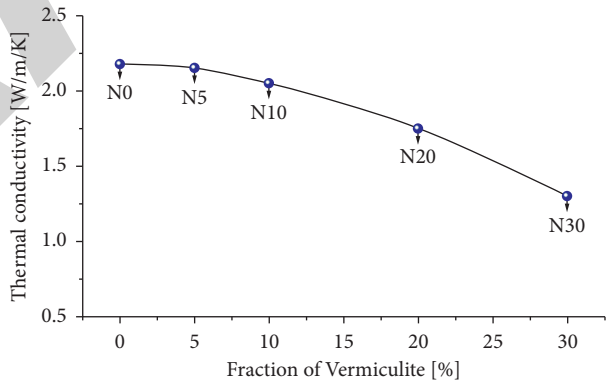

Figure 5: Thermal conductivity of normal concrete. On increasing the fraction of vermiculite, k decreases.

conductivity of 2.175 W/m/K is observed for concrete without addition of vermiculite. Thermal conductivity decreases to 1.30 W/m/K as the amount of vermiculite increases (accordingly the volume of coarse aggregate decreases), which is approximately 43% reduction at 30% of vermiculite (N30 specimen). To prevent the exclusion of coarse aggregates, addition of vermiculite is limited to not more than 30%.

Figure 6 depicts the thermal conductivity of pumice concrete specimens [P series] vs. normal aggregate concrete specimens. Pumice has a higher porosity and hence a superior heat conductivity. Vermiculite is added to the concrete mixture to produce mechanical fineness and strength. Furthermore, when the volume percentage of vermiculite is raised from 0 to 20%, the conductivity of the pumice concrete specimens drops to 30%.

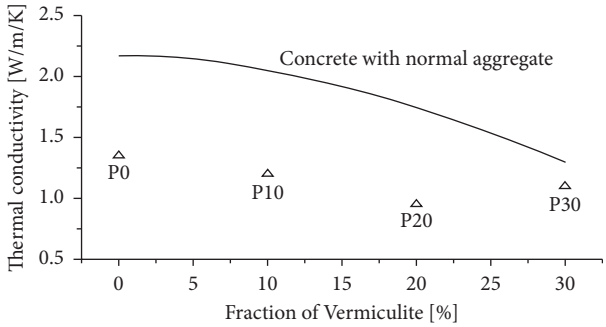

Figure 6: Thermal conductivity of concrete with pumice aggregates. Increase in vermiculite by 20% caused a 30% decrease in thermal conductivity, k.

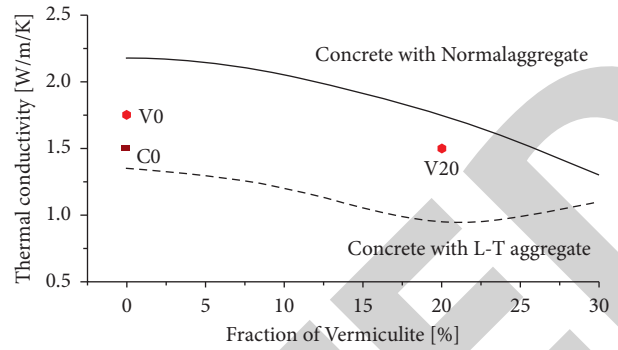

Figure 7: Thermal conductivity of coconut shell and volcanic rock concretes.

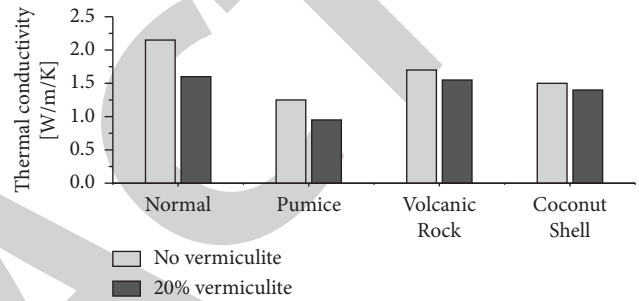

Figure 8: Thermal conductivity of concrete specimens with and without 20% vermiculite content.

Figure 7 compares the thermal conductivity of volcanic rock and coconut shell concretes to that of normal and pumice concretes. The solid line represents the heat conductivity of normal concrete as the vermiculite proportion increases. The dotted line is used to symbolize the same thing as the pumice (P series) concrete. The thermal conductivity of the volcanic rock concrete specimen V0 is 1.75 W/m/K. The thermal conductivity of the specimen was lowered to 1.5 W/m/K after the addition of 20% volume of vermiculite. Thermal conductivity decreases by 14% as vermiculite volume increases. Thermal conductivity values for C0 and V20 are comparable. However, vermiculite is not added to coconut shell concretes to ensure the fineness of the mechanical qualities. It is worth noting that pumice has the lowest heat conductivity. Pumice specimens with 20% vermiculite exhibit the lowest thermal conductivity.

The comparison between specimens without vermiculite and with 20% of vermiculite for four different aggregates specimens is shown in Figure 8. As justified earlier, adding 20% vermiculite, there is an effective improvement in reducing thermal conductivity in specimens with normal and pumice as coarse aggregates.

3.2. Effective Range of the Thermal Needle Probe Method. The needle probe is inserted into the concrete specimen prior to hardening and provides radial heat into the specimen up to a certain reach. Because the needle probe is lodged inside the concrete specimen throughout the casting process, the recorded value at various temperature ranges reflects the material characteristics within the effective volume. The quantity of heat created by the probe is measured using thermocouples encased within the concrete specimen, and thermal conductivity is computed using equation (1). The main disadvantage of this approach is that the heat generated is not completely disseminated through the block; hence, the thermal moulding method is used.

3.3. Results from the Thermal Molding Method. The temperature change with time for four distinct specimens is depicted in Figure 9 using thermocouples within the specimen. The temperature difference between the specimen and the heating plate is represented by the red line. Based on the equation, experimental findings are represented by solid lines, while temperature is denoted by dotted lines (2). When the plate begins to heat, the temperature rises quickly and reaches 600 degrees Celsius. The temperature rises steadily from the first thermocouple to the heating plate. During transitory times, a lag is seen.

The temperature rises at each thermocouple in turn. Unless there is no heat loss, there is a coincidence between the thermocouple temperature and the asymptotic value at steady state. Despite insulating, temperature changes at steady state are observed owing to heat loss to the environment. The heat loss coefficient is sufficient to account for the temperature rise at four thermocouples over time. Thermal conductivity measured by thermal moulding and the needle probe techniques agrees well in Figure 10, demonstrating the importance of coarse particles and vermiculite. Low specific heat leads to poorer conductivity in the thermal moulding analysis because thermal conductivity has a reciprocal and linear connection. Table 8 highlights the specific heat values of several concrete materials, which range from 795 to 1000 J/kg/K. The temperature evolution throughout the transient period from the needle probe method may be used to calculate the specific heat value. Figures 11 and 12 show the density of specimens as a function of the percent of vermiculite used, as well as the compressive strength as a function of the fraction of vermiculite used.

3.4. Results from the One-Dimensional Heating Method. The temperature readings by the thermocouples for the corresponding concrete specimens are plotted. Figure 13(a))

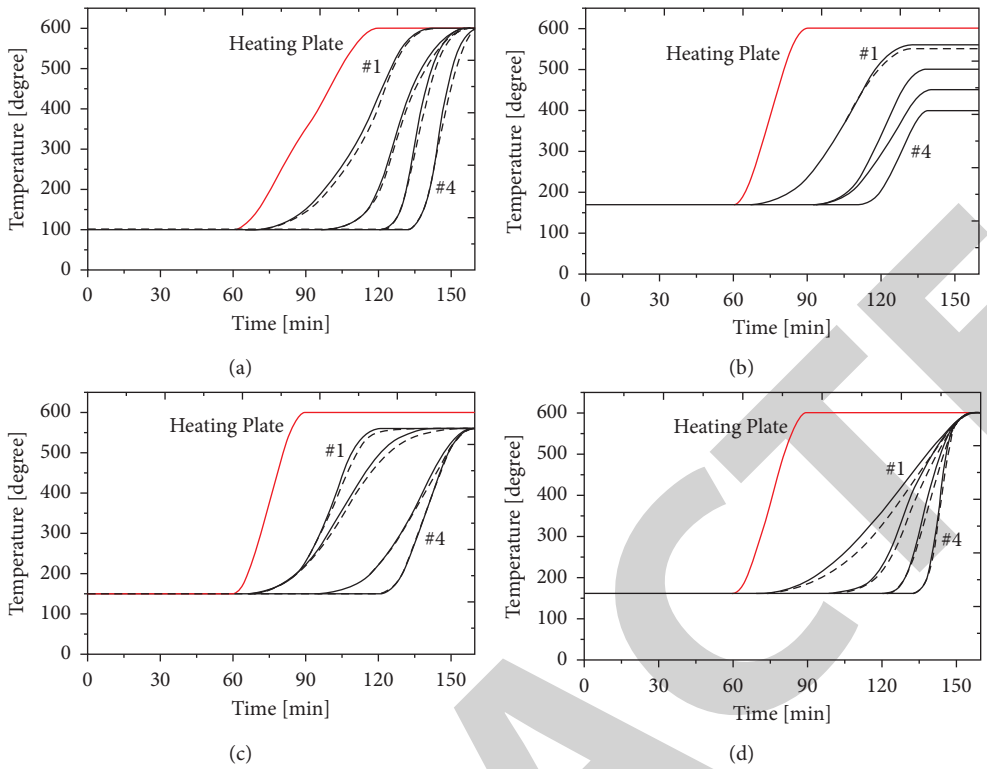

Figure 9: Temperature evolution of (a) *N*0, (b) *N*10, (c) *N*30, and (d) *P*20 specimens with time. Solid lines (experimental results) and dotted lines (evaluated temperature). Reddish colored line.

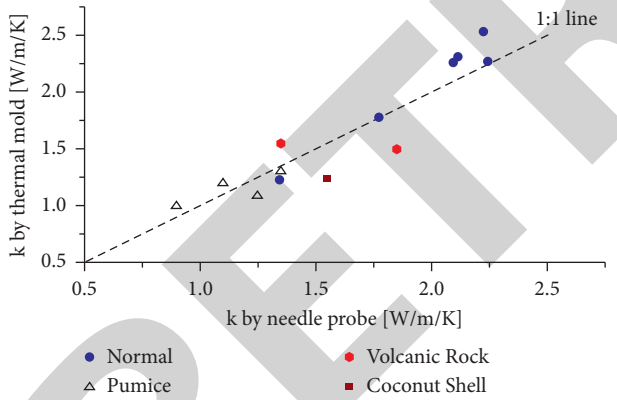

Figure 10: Thermal conductivity by the thermal needle probe and thermal molding methods.

shows the temperature readings by the thermocouples in normal aggregates specimens (*N* series). Each composition is designated by different symbols for better clarity. The thermocouples are denoted by *T* along with the number of their positions (*T*1, *T*2.etc.).When studied, it is noted that the N30 specimen shows low thermal conductivity among the other specimens in the N series when 30% fraction of vermiculite is added to the mixture. In Figure 13(b)), temperature recorded from the thermocouples from pumice concrete specimens is plotted. Among all the specimens, an efficient reduction in heat flow is demonstrated by the P20 specimen. Pumice acts as an excellent insulator at higher temperatures.

Figure 13(c)) shows the temperature values of the volcanic rock specimens V0 and V20. From the two specimens, V20 shows lower thermal conductivity than V0. Here, heat propagation is further reduced by the addition of vermiculite. Figure 13(d)) shows temperature depreciation throughout the C0 specimen recorded from the thermocouples. From the above figure, it is distinctive that among all the specimens, P20 specimen has the lowest thermal conductivity and hence provides better insulation than the rest.

3.5. Applications of Thermo-Shielding Concretes. Table 8 highlights the mechanical characteristics of hardened concrete after 28 days of curing. Normal concrete density fluctuates by around 15% from 2389 kg/m^3 in *N*0 to 2023 kg/m^3 in *N*30 when vermiculite is substituted up to 30%. According to Figure 10, the addition of vermiculite in volume has no significant effect on the density reduction in other LWAC. Except for the combination containing 30% vermiculite, all mixes achieve a 28-day cylindrical compressive strength of 28 MPa. The compressive strength of normal and LWAC concretes decreases significantly as the vermiculite replacement volume increases; however, the change in compressive strength and the density of coconut shell concretes is negligible. The modulus of elasticity and splitting tensile strength have comparable properties to density and compressive strength. The distribution and the size of LWAs have a significant impact on the mechanical characteristics of concrete.When applied to structural

Table 8: Mechanical properties at 25 days.

Specimen	Density (kg/m^3)	Compressive strength (MPa)	Modulus of elasticity (GPa)	Splitting tensile strength (MPa)
*N*0	2389	44.2	42.65	4.25
*N*5	2300	39.7	37.32	3.64
*N*10	2260	37.4	35.05	3.14
*N*20	2169	33.1	33.25	2.35
*N*30	2023	27.5	24.94	2.12
*P*0	1854	39.6	28.95	3.47
*P*10	1833	38.8	27.82	3.22
*P*20	1801	32.0	24.36	2.95
*P*30	1796	27.8	20.42	2.06
*V*0	1864	40.5	25.68	3.84
*V*20	1837	36.3	22.81	3.18
*C*0	1826	39.9	27.64	3.23

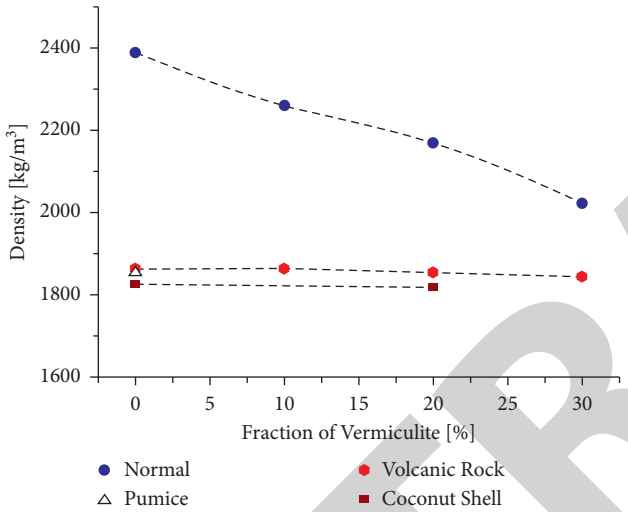

Figure 11: Density of specimens with a fraction of vermiculite.

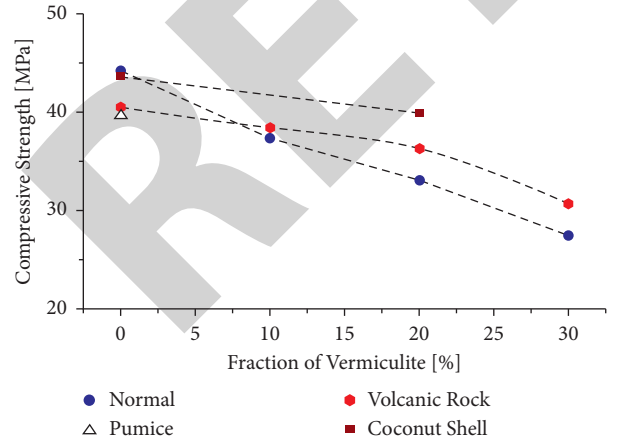

Figure 12: Compressive strength with a fraction of vermiculite.

elements such as the wall of a nuclear reactor safety vessel, the mechanical characteristics of insulated concrete with LWA and vermiculite meet the fundamental standard and code of building construction.

3.6. LWA Vermiculate Concrete. The RV model, as illustrated in Figure 14, is a scaled replica of a genuine RV in a nuclear reactor. It is built out of a cylindrical block of high strength concrete with a CS pipe running through the middle. The concrete block is 10 inches in diameter and 12 inches in length. The CS pipe has a diameter of 1 inch and a length of 18 inches. Both ends of the CS pipe are joined to a flange, which connects it to the external setup. The RV model is then attached to the external setup, which circulates the heat transfer fluid (water) at a higher temperature. The heat emitted by the water is collected by the tubes and conveyed through the concrete.

3.7. Fabrication of the RV Model. A appropriate mould made of LWA vermiculite is created in order to produce the cylindrical concrete block. The fundamental reason for this is because various building materials require varied amounts of time to set. Although the introduction of additives or admixtures changes the setting time of concrete, it is still required to ensure that the concrete maintains its right form. A PVC block with a diameter of 10" is utilized as the outer boundary, a CS pipe with a diameter of 1″ passes through the middle of the PVC coupling, and a wooden board is used to close one of the apertures. Once the concrete has cured, the LWA vermiculite concrete mould is removed.

3.7.1. Experiment Procedure for the RV Model. The RV model is attached to the external setup by a flange, which is a square portion with mounting holes drilled in it. The CS pipe flowing through the RV model is likewise provided via a flange with the same size as the exterior configuration. An external setup interface gasket is supplied to prevent leaking at the RV. The reservoir is normally filled with the heat transfer fluid, which is water. With the assistance of an immersion heater, it is heated to a temperature of 60°C. The fluid flow rate is regulated and maintained at the desired level. Flow rate is determined with a flowmeter. As hot water circulates through the circuit, the concrete gradually warms up. Temperature measurements are recorded and tabulated every 5 minutes at each thermocouple. After a set period of time, the RV model reaches a steady state and there is no additional temperature growth.

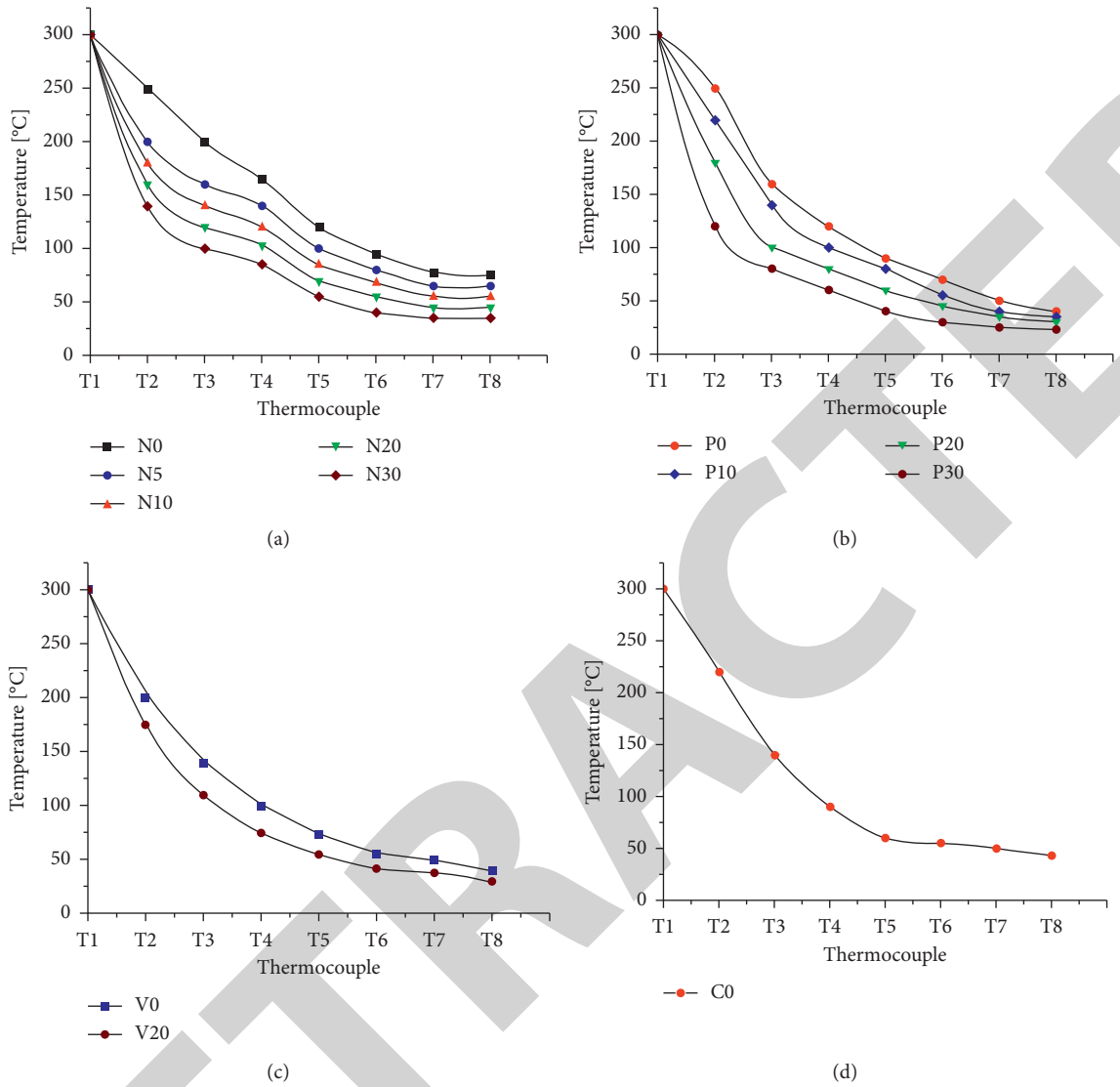

Figure 13: Temperatures across the thermocouples of (a) normal aggregates, (b) pumice aggregates, (c) volcanic rock, and (d) coconut shell aggregate specimens.

3.8. Convective Heat Transfer through Pipe and Concrete Surface. The photographs demonstrate the many steps of heat transmission from water to the concrete surface. Convective heat transfer from hot water to the pipe is seen in Figure 14. The average temperature of the water flowing through the pipe was determined to be 56°C, since heat is transferred from the water to the pipe surface as it runs. It can be observed that the pipe temperature at the intake is near to the water temperature, as indicated in red, and progressively decreases as they approach towards the exit, as shown in green. Heat from the pipe surface is transmitted to the outside surface of the RV model by convection as the exterior setup is exposed to the environment, as shown in Figure 15. Although conduction accounts for the majority of heat transmission through concrete, the action of air movement over the concrete surface also transmits heat. Because the region near the pipe absorbs heat faster than the outermost surface, the color variation ranges from orange at the start to deep blue at the finish. The RV model is analyzed using ANSYS software to explore the heat transfer properties through the concrete material in detail. Because the project's fundamental principle is heat transmission via conduction, the entire RV model is broken into minute nodes by meshing. The notion of meshing is the development of a grid across an entire model in order to analyze parameters such as temperature, heat flow, and temperature gradient at specified spots on the model known as nodes, and the results are obtained.

3.9. ANSYS Thermal Gradient and Thermal Flux Vector Sum. When the intake circumstances are supplied as input, this graphic displays the thermal gradient values along all three axes (x, y, and z) of the RV model. It is obvious that the temperature gradient values adjacent to the pipe are large, with a value of 702.18 W/m, and have a minimum value of

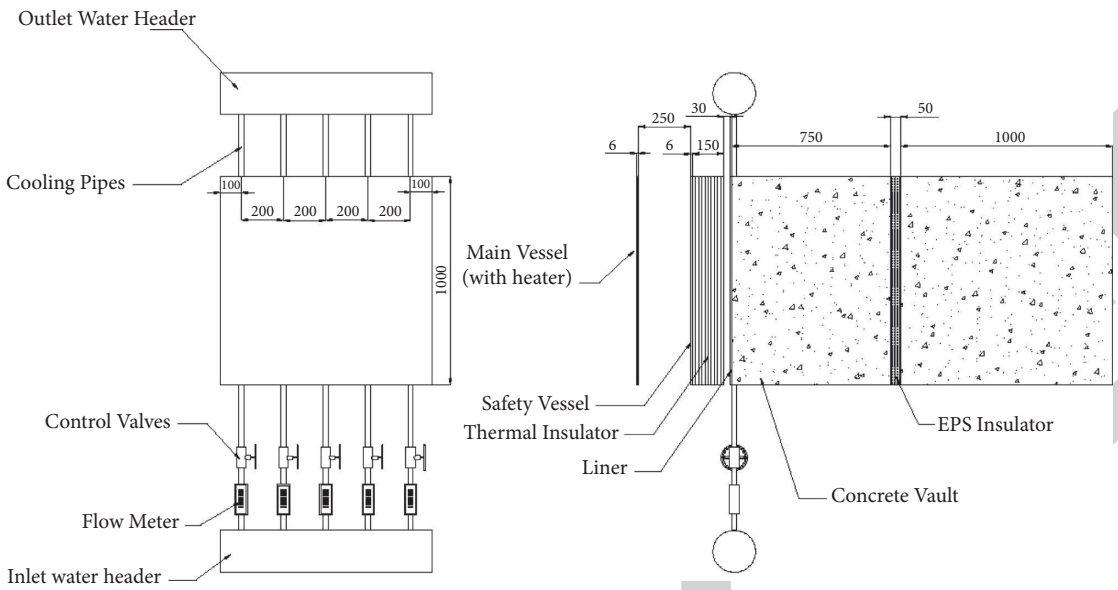

Figure 14: Concrete reactor vault.

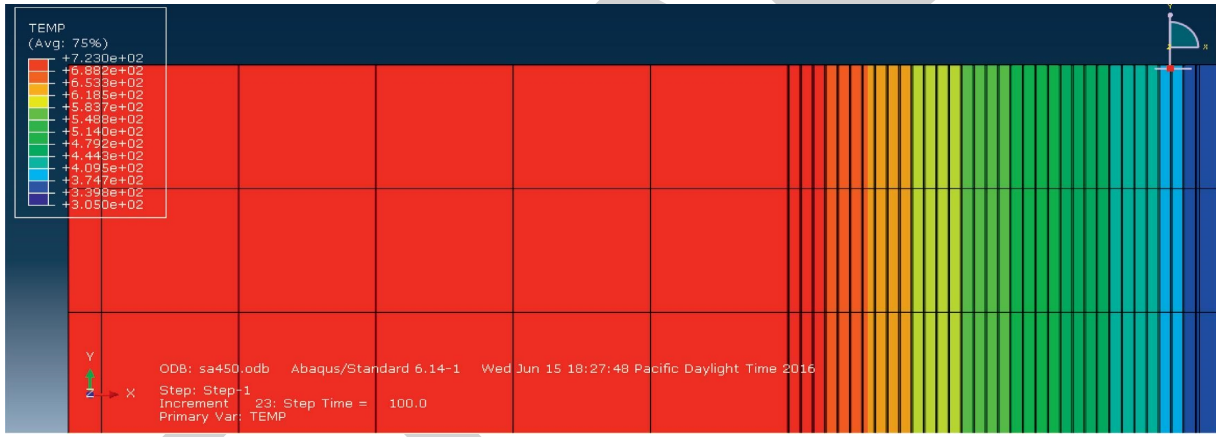

Figure 15: Convective heat flow through the CS pipe and the concrete layer.

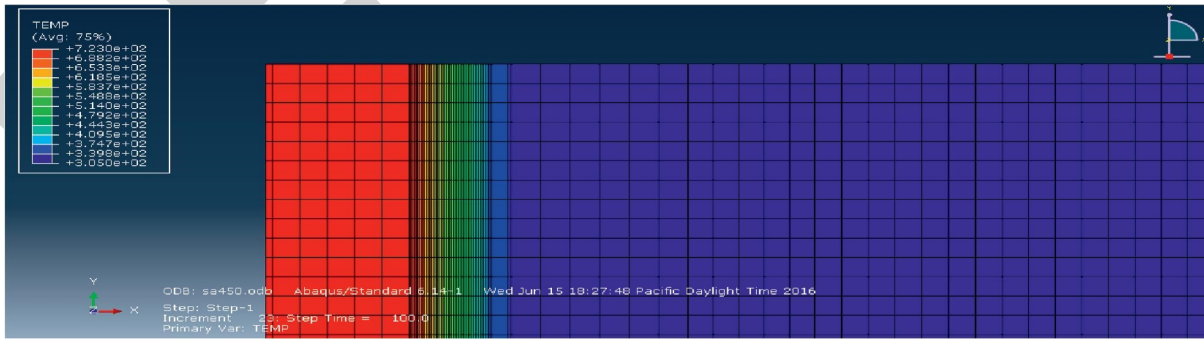

Figure 16: Showing thermal gradient for nodal solution.

75.98 W/m on the outside surface. As we go closer to the surface, the thermal gradient values become more similar to air conditions. Figure 16 depicts the results of the investigation into heat movement through the cylindrical concrete block as well as convection into the surrounding area. There were nodes in the centre area and on the surface that had the largest heat flow, and there were nodes on the block that had the lowest heat flow, with the maximum value being 1098.93 W/m^2. x-axis heat flux for the nodal solution is negative, with a value of 1097.88 denoting the direction

opposed to the flow against the previously assumed direction, with a maximum value of 1098.93 W/m^2 in the centre and a value of −121.639 W/m^2 as it approaches the outside walls.

4. Conclusion

Experimentally determined thermal conductivity values for thermally insulated concretes with lightweight aggregates and vermiculite as substitute materials are investigated, and the findings are explained.

(1) To validate the reliability of the estimated values in terms of application, results from the thermal needle probe technique and thermal moulding testing in one- and two-dimensional heat flow are experimented with.

(2) The replacement of conventional aggregate with the LWAs effectively diminishes thermal conductivity subjected to the raw materials.

(3) Coarse particles have a stronger impact than exfoliated vermiculite. In this investigation, pumice with a conductivity of 0.9 W/m/K on 20–30% vermiculite was shown to be the most effective insulating addition.

(4) To ensure mechanical soundness, the addition of vermiculite is restricted to not more than 20%. The quantitative value of the thermal conductivity evaluated at high temperatures becomes a vital factor to simulate and analyze the thermal behavior of the nuclear reactor safety vault built from these lightweight aggregate concretes.

(5) The high strength concrete was cast according to the design mix. The experiment was carried out on the setup, calculations were done, and the values were validated using ANSYS software. Thermal conductivity (K) values for mild steel pipe and high strength concrete material were determined to be 53.3717 W/mK and 1.56503 W/mK, respectively, which were found to be consistent with theoretical values.

(6) When the temperature of the main vessel (heater plate) is set at 100°C, the temperature difference between the inner (T49) and outer faces (T55) of the inner concrete vault is 3°C, which is less than the acceptable temperature difference. At 200°C, the temperature difference between the inner (T49) and outer faces (T55) of the inner concrete vault is 5°C, which is less than the acceptable temperature difference. At 300°C, the temperature difference between the inner (T49) and outer faces (T55) of the inner concrete vault is 7°C, which is less than the acceptable temperature difference. At 400°C, the temperature difference between the inner (T49) and outer faces(T55) of the inner concrete vault is 13°C, which is less than the acceptable temperature difference. At 500°C, the temperature difference between the inner (T49) and outer faces (T55) of the inner concrete vault is 21°C, which is less than the acceptable temperature difference.

(7) When the temperature of the main vessel (heater plate) was set to 57^{7}°C, the temperatures of the inner and outer faces of the inner concrete vault were 7^{1}°C (T49) and 4^{7}°C (T55), respectively, with a difference of 24°C, which was less than acceptable when using thermally insulated concretes with lightweight aggregates and vermiculite as alternate materials.

(8) Thermal conductivity was found to be lower in plain concrete of grades N0, N5, and lightweight aggregates concrete, with conductivities of 1.65 W/mK, 1.59 W/mK, and 1.703 W/mK, respectively. This implies that the lightweight aggregates vermiculate concrete composition retains the heat energy transmitted by conduction from the pipe without letting it to distribute heat to the surrounding environment.

Data Availability

The data used to support the findings of this study are included within the article. Further data or information is available from the corresponding author upon request.

Conflicts of Interest

The authors declare that there are no conflicts of interest regarding the publication of this paper.

Acknowledgments

The authors thank MizanTepi University, Ethiopia, for providing help during the research and preparation of the manuscript. The authors thank the Sathyabama Institute of Science and Technology, CMR Institute of Technology, and Seoul National University of Science and Technology, for providing assistance to complete this work. This project was supported by Researchers Supporting Project number (RSP-2021/315) King Saud University, Riyadh, Saudi Arabia.

References

[1] K. Y. Shin, S. B. Kim, J. H. Kim, M. Chung, and P. S. Jung, "Thermo-physical properties and transient heat transfer of concrete at elevated temperatures," *Nuclear Engineering and Design*, vol. 212, no. 1-3, pp. 233–241, 2002.

[2] A. Saygılı and G. Baykal, "A new method for improving the thermal insulation properties of fly ash," *Energy and Buildings*, vol. 43, no. 11, pp. 3236–3242, 2011.

[3] L. H. Nguyen, A. L. Beaucour, S. Ortola, and A. Noumowé, "Experimental study on the thermal properties of lightweight aggregate concretes at different moisture contents and ambient temperatures," *Construction and Building Materials*, vol. 151, pp. 720–731, 2017.

[4] C. Tasdemir, O. Sengul, and M. A. au, "A comparative study on the thermal conductivities and mechanical properties of lightweight concretes," *Energy and Buildings*, vol. 151, pp. 469–475, 2017.

[5] K. Gunasekaran and P. S. Kumar, "Lightweight concrete using coconut shells as aggregates," in *Proceedings of the*

international conference on advances in Concrete and construction, pp. pp450–459, Washington DC, October 30, 2008.

[6] K. H. Kim, S. E. Jeon, J. K. Kim, and S. Yang, "An experimental study on thermal conductivity of concrete," *Cement and Concrete Research*, vol. 33, no. 3, pp. 363–371, 2003.

[7] T. D. brown and M. Y. javaid, "The thermal conductivity of fresh concrete," *Matériaux et Constructions*, vol. 3, no. 6, pp. 411–416, 1970.

[8] T. S. Yun and Y. J. T.-S. K.-S. Jeong, "Evaluation of thermal conductivity for thermally insulated concretes," *Energy and Buildings*, vol. 61, pp. 125–132, 2013.

[9] H. K. Kim, J. H. Jeon, and H. K. Lee, "Workability, and mechanical, acoustic and thermal properties of lightweight aggregate concrete with a high volume of entrained air," *Construction and Building Materials*, vol. 29, pp. 193–200, 2012.

[10] S. Widodo, F. Ma'arif, B. S. Gan, and B. S. Gan, "Thermal conductivity and compressive strength of lightweight mortar utilizing Pumice breccia as fine aggregate," *Procedia Engineering*, vol. 171, pp. 768–773, 2017.

[11] M. Davraz, M. Koru, and A. E. Akdağ, "The Effect of Physical properties on thermal conductivity of lightweight aggregate," *Procedia Earth and Planetary science*, vol. 15, pp. 85–92, 2015.

[12] A. Narayanan and P. Shanmugasundaram, "An experimental investigation on flyash-based geopolymer mortar under different curing regime for thermal analysis," *Energy and Buildings*, vol. 138, pp. 539–545, 2017.

[13] O. Sengul, S. F. Azizi, and M. A. au, "Effect of expanded perlite on the mechanical properties and thermal conductivity of lightweight concrete," *Energy and Buildings*, vol. 43, no. 2-3, pp. 671–676, 2011.

[14] H. Kallel, H. Carré, C. La Borderie, B. Masson, and N. C. Tran, "Effect of temperature and moisture on the instantaneous behaviour of concrete," *Cement and Concrete Composites*, vol. 80, pp. 326–332, 2017.

[15] L. Shen, R. Q. Zhang, L. Zhang, Y. Han, G. Cusatis, and G. Cusatis, "Experimental and numerical study of effective thermal conductivity of cracked concrete," *Construction and Building Materials*, vol. 153, pp. 55–68, 2017.

[16] S. Divya Rani and M. Santhanam, "Influence of moderately elevated temperatures on engineering properties of concrete used for nuclear reactor vaults," *Cement and Concrete Composites*, vol. 34, no. 8, pp. 917–923, 2012.

[17] P. R. Kalyana Chakravarthy, R. Janani, T. Ilango, and K. Dharani, "Properties of concrete partially replaced with coconut shell as coarse aggregate and steel fibres in addition to its concrete volume," *IOP Conference Series: Materials Science and Engineering*, vol. 183, Article ID 012028, 2017.

[18] W. Zhang, H. Min, X. Gu, and Y. Y. Xi, "Mesoscale model for thermal conductivity of concrete," *Construction and Building Materials*, vol. 98, pp. 8–16, 2015.

[19] L. H. Nguyen, A.-L. Beaucour, S. Ortola, and A. Noumowé, "Influence of the volume fraction and the nature of fine lightweight aggregates on the thermal and mechanical properties of structural concrete," *Construction and Building Materials*, vol. 51, pp. 121–132, 2014.

[20] M. Sutcu, "Influence of expanded vermiculite on physical properties and thermal conductivity of clay bricks," *Ceramics International*, vol. 41, no. 2, pp. 2819–2827, 2015.

[21] Ö. S. Bideci, "The effect of high temperature on lightweight concretes producedwithcolemanite coated pumice aggregates," *Construction and Building Materials*, vol. 113, pp. 631–640, 2016.

[22] A. Kanojia and S. K. Jain, "Performance of coconut shell as coarse aggregate in concrete," *Construction and Building Materials*, vol. 140, pp. 150–156, 2017.

[23] I. Budaiwi and A. Abdou, "The impact of thermal conductivity change of moist fibrous insulation on energy performance of buildings under hot-humid conditions," *Energy and Buildings*, vol. 60, pp. 388–399, 2013.

[24] M. Anish, B. Kanimozhi, S. Ramachandran, and J. N. Jayaprabakar, "Analysis of heat transfer through a high strength concrete with circular pipe in a safety vessel of reactor vault," *International Journal of Ambient Energy*, vol. 39, no. 7, pp. 678–684, 2017.